Reduction of Drag Rise on the Convair 990 Airplane

JOHN T. KUTNEY*
General Electric Company, Cincinnati, Ohio

AND

STANLEY P. PISZKIN†
General Dynamics, San Diego, Calif.

The drag rise Mach number of the Convair 990 airplane was significantly delayed by utilizing the area-rule principle in a manner not previously reported in the literature. The principle was applied locally to the nacelle-pylon-wing region in a full-scale flight test to improve the maximum speed capability. The results of the full-scale investigations which led to the final airplane configuration are presented. The final modifications to the aircraft for delaying the drag rise included a forward pylon fairing, an aft pylon fairing, and four terminal fairings added to the inboard sides of the nacelles. This configuration was incorporated into the final airplane design without major aircraft redesign or modification. The methods employed to identify and isolate the interference drag phenomena on the airplane and the analytical approach to the problem solution are explained. The results and data analysis include the incremental effects of the various modifications, surface pressure distributions, stabilized speed point data, and pilot observations on Mach buffet characteristics. A criterion was established which will add to the fundamental understanding of the causes of interference drag and the methods for alleviating the resultant drag rise. Examples of configurations suggesting potential application of the technique are pylon-mounted engine nacelles on wings or fuselages and externally mounted stores.

Introduction

THE Convair Model 990 is an advanced version of the Convair Model 880 and is a medium range swept-wing four-engine turbofan transport powered by four General Electric aft-fan engines. An extensive drag reduction program on the 990 was initiated when early flight tests revealed that compliance with cruise performance guarantees could not be demonstrated. The program consisted of three general phases: 1) exploratory flight tests, 2) an extensive engine nacelle wind tunnel investigation, and 3) development flight tests. Modifications of the following nature were established: 1) a sharper, less drooped, wing leading edge, 2) a nacelle afterbody extension, 3) a wing-fuselage aft fillet redesign to more generous lines, and 4) the addition of engine nacelle and pylon fairings. The incorporation of these modifications has resulted in the achievement of cruise performance in excess of the original guarantees. Modifications 1, 2, and 3 were established from the first two phases of the program; whereas the nacelle and pylon fairings were developed during the flight-test phase. This final phase, in which the airplane drag rise was markedly reduced as a result of a local application of the area-rule technique to the nacelle-pylon-wing regions, is the subject of this paper.

Statement of the Problem

The initial nacelle-pylon configuration of the flight-test development phase is shown in Fig. 1. The nacelle afterbody extension and the wing leading-edge modification which were established during the previous phases are incorporated in this configuration. Although improvement was attained with these modifications, maximum speed performance remained deficient.

Presented as Preprint 63-276 at the AIAA Summer Meeting, Los Angeles, Calif., June 17–20, 1963; revision received December 4, 1963.

* Manager, Applications and Installations, V/STOL Systems Operations.

† Senior Aerodynamics Engineer, Convair.

During the initial phase of the full-scale flight-test program, complete nacelle afterbody pylon and wing surface pressure distributions were obtained with a scannivalve type system. These data were reduced and analyzed within 24 hr after each flight. Examination of these pressure data indicated the presence of local supersonic flow fields at aircraft flight speeds of $M = 0.8$–0.9. The nacelle boattail pressure peaks were considerably more negative than would be obtained on the same nacelle geometry acting as an isolated body. A considerable variation of these pressures existed in the meridianal planes with the levels getting progressively more severe near the nacelle pylon junction. The nacelle boattail pressure distributions presented in Fig. 2 illustrate these observations. There was a noticeable uniformity of pressure distributions for the wing lower surface and nacelle upper surface as shown in Fig. 3. This strong uniformity and characteristic independence of each side of each nacelle is indicative of a strong local interference flow phenomenon. The integration of these pressures for the nacelle afterbodies yielded pressure drag levels and drag rise characteristics considerably higher than should be expected for isolated bodies of the same geometry. The afterbody pressure drag breakdown for this original configuration is presented in Fig. 4.

A comparison of total afterbody pressure drag rise with airplane drag rise is presented in Fig. 5. This correlation provided the basis for the continued flight-test development effort. This analysis indicated that the total aircraft drag rise up to approximately $M = 0.88$ was confined to the nacelle, pylon, and wing region and that elimination of this local drag rise would result in the elimination of the total aircraft drag rise up to that Mach number, more than required to satisfy the speed requirement.

Method of Approach

The uniformity of the pressure distributions for the wing lower surface and the nacelle upper surface shown in Fig. 3 (particularly on the inboard sides of the nacelles) suggested that the flow could be treated as one dimensional in the local regions bounded on three sides by the wing lower surface, the sides of the pylon, and the nacelle upper surface. Pre-

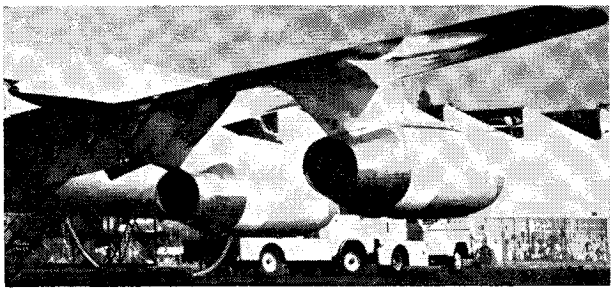

Fig. 1 Convair 990 with unmodified pylon and nacelle.

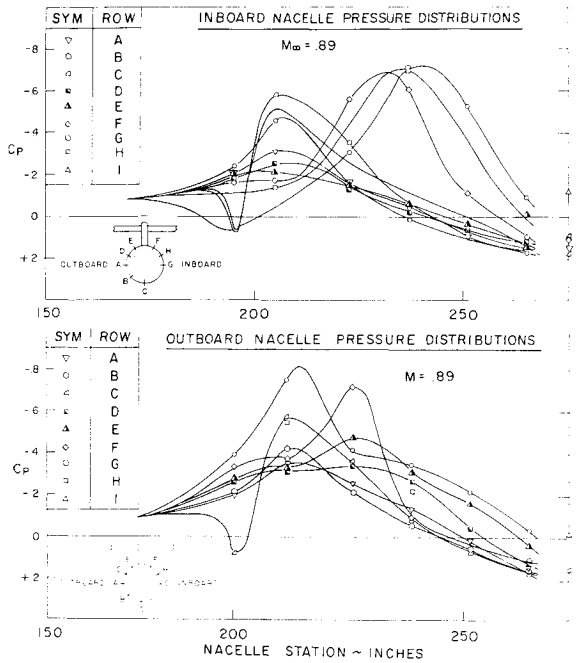

Fig. 2 Nacelle pressure distributions.

sented also in Fig. 3 is a correlation of pressure data with simple one-dimensional flow models for the inboard side of the inboard nacelle. The two cases considered are identified by the accompanying sketch as: 1) a one-dimensional channel defined by the surface contours along the two pressure rows and 2) a three-dimensional channel defined by the cross-hatched area. The theoretical pressure distributions are developed only for the supersonic expansion aft of the assumed sonic throat without attempting to define the shock and separation region. Note that both of the flow models correlate well with respect to axial station location and pressure gradient. Similar results are obtained for the remaining sides of the nacelles, except that less correlation is obtained for the outboard sides where the pressure gradients and peaks are less pronounced.

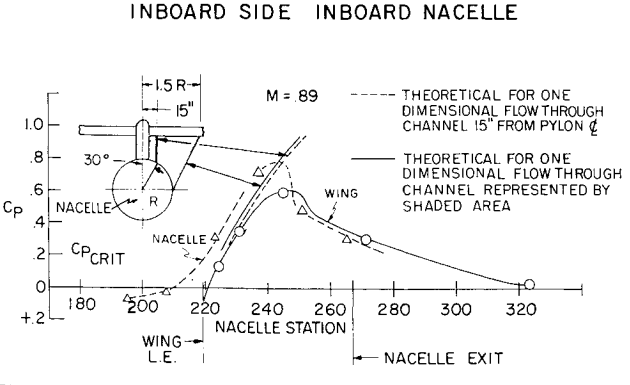

Fig. 3 Comparison of pressure distribution with theoretical one-dimensional flow models.

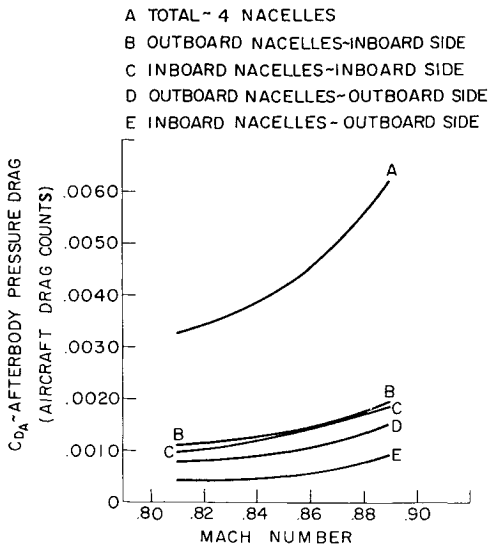

Fig. 4 Nacelle afterbody drag breakdown based on pressure distributions initial modification configuration.

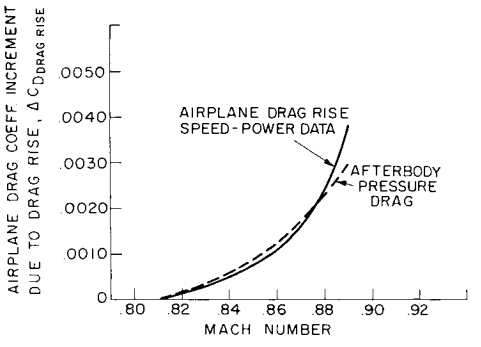

Fig. 5 Comparison of nacelle afterbody drag rise with speed-power data.

The degree of correlation obtained with the one-dimensiona flow analogy prompted the employment of an area-distribution technique to eliminate the supersonic flow conditions. The application of this technique was broken down into three steps:

1) Establishment of cross-section boundaries for the area-distribution cuts.

2) Definition of desired area distributions.

3) Determination of the particular geometry.

The flight test program was redirected (based on these conclusions) to obtain the information required to develop the technique and, ultimately, the final solution.

The area-distribution boundary conditions employed throughout the program are illustrated in Fig. 6. The logic used in establishing these boundaries is as follows:

1) Near-sonic flow conditions preclude interaction effects across a plane surface as a wing except very near the leading edge, and only the wing lower surface was included in the area distribution.

2) At low wing lift coefficients (as was the case for the high-speed, light-weight condition under consideration) the wing stagnation streamline lies nearly in a plane surface parallel to the freestream flow direction and intersecting the wing along the leading edge line. This plane surface was used as the upper boundary. Since thrust axes are very nearly parallel to the flight direction for the flight condition under consideration, they were used as the reference direction.

3) Similar to the reasoning of item 2, a vertical plane surface bisecting the nacelle and pylon was used as a side boundary. The pressure data clearly illustrated the asymmetry of flow across the pylon necessitating separate treatment of each side of each nacelle.

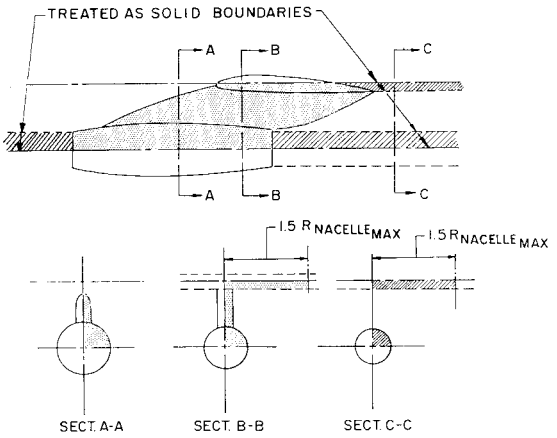

Fig. 6 Initial area distribution boundaries applicable to each side of each nacelle.

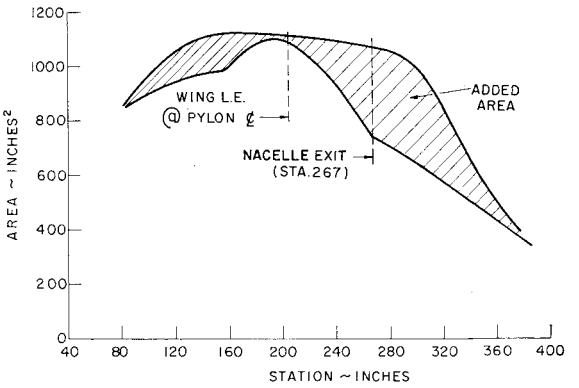

Fig. 8 Illustration of concept of desired distribution modification.

4) As shown in Fig. 2, nacelle afterbody pressures indicated a definite decrease in the negative peaks from the upper quadrant to the lower quadrant thus suggesting that the interference phenomenon did not extend all the way around the nacelle. Only the upper quadrant was included in the area distribution defining a plane surface parallel to the upper boundary and passing through the nacelle centerline as the lower boundary.

5) The jet exhaust was treated conventionally as a solid circular cylinder in the area distribution.

6) Insufficient pressure data existed to determine precisely the spanwise extent of the interference disturbance near the pylon. However, pressure data at wing stations 30 in. inboard of each pylon centerline ($0.85^R\text{pod}_{\max}$) showed the disturbance to be only slightly attentuated at this station. Therefore, some greater dimension than 30 in. was indicated for the spanwise boundary. A boundary line 1.5 times the maximum nacelle radius ($1.5^R\text{max}_{\text{pod}}$) away from the pylon centerline was selected.

Area distributions for the initial configuration are presented in Fig. 7 for each side of each nacelle. The wing leading edge and pod exit stations are identified to indicate the extent of wing-nacelle overlap for each case. Note that the inboard sides are characterized by a noticeable area peak with large curvature in the overlap region, whereas the outboard sides are not. The pressure distribution and integration of Fig. 2 indicated that the major drag problem was associated with the inboard sides as would be expected from observation of the area distributions.

The determination of desired area distributions as well as acceptable geometries was an iterative process through successive flight tests. The primary approach was to reduce the marked area curvature occurring at the peak-area points on the inboard sides of the nacelle. The axial location of these peaks on the aircraft coincided with primary pylon structuer.

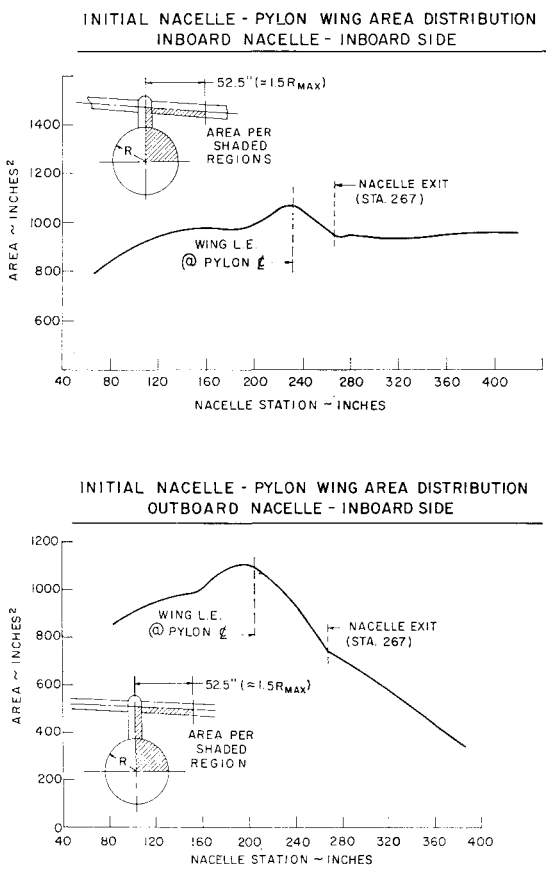

Fig. 7 Initial nacelle-pylon wing area distribution.

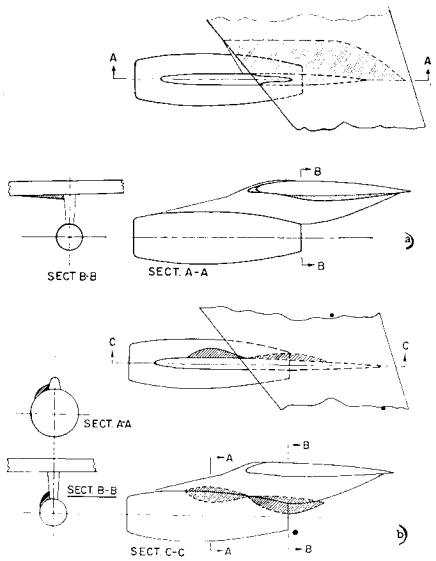

Fig. 9 a) Wing leading edge and lower surface fairing concept; b) nacelle fairing concept.

This fact, coupled with the need to retain the existing wing and nacelle basic structure, necessitated adoption of the concept of adding area forward and aft of the peak-area point as illustrated in Fig. 8. The general concepts which were considered fall into three categories: pylon fairings, nacelle fairings, and wing leading edge and lower surface fairings. Typical illustrations of these concepts are presented in Figs. 9 and 14.

Results

Several combinations and variations of the three basic concepts were defined and tested in a full-scale mock-up flight-test program. Area distributions for these various modifications are presented in Fig. 10. The resultant drag improvements are presented in Fig. 11. Associated with the progressive drag-rise reduction was the observation that

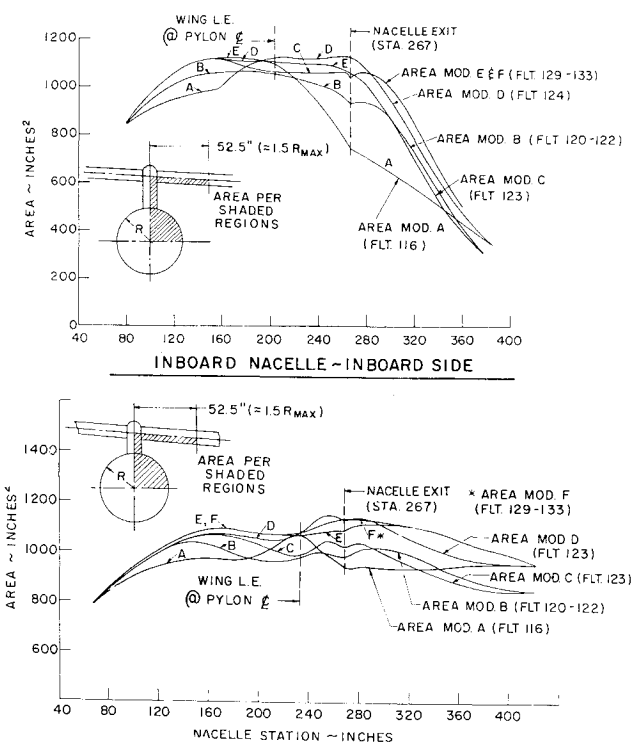

Fig. 10 Nacelle-pylong wing area distributions.

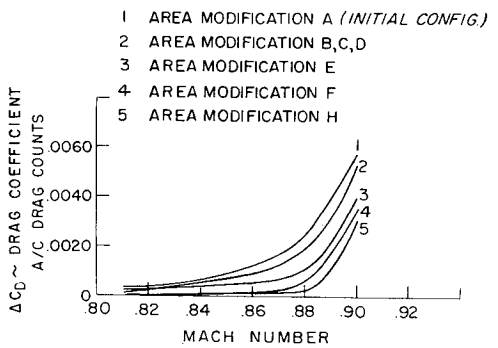

Fig. 11 Effect of area distribution modifications.

correspondingly higher buffet onset speeds were reported by the test pilots thus providing further confidence in the method of attack.

Correlation of key pressure levels with area-distribution curvature was established as shown in Fig. 12. Of significance is the fact that two phenomena exist, one for the confined flow region from the wing leading edge to the nacelle exit, and another for the unconfined region aft of the exit. Based on this correlation, one-dimensional pressure distributions were estimated and integrated for a series of arbitrary area distributions in attempts to define optimal shapes.

Integration of nacelle afterbody pressures to obtain component drag breakdowns was used throughout the program. The summary data presented in pressure drag integration form in Fig. 13 illustrates the changes in drag level and drag rise resulting from the various area modifications.

The most effective and final production configuration is illustrated in Fig. 14. The resultant data analysis included a breakdown of the individual modifications; the aft pylon fairings, the forward pylon fairings, and the nacelle terminal fairings as illustrated in Fig. 15. The unmodified pylon and nacelle sections illustrated in Fig. 1 show considerable difference in geometry compared to Fig. 16 with the thickened aft pylon section and variations of terminal fairings used in the program.

Generalization

Although the information reported herein is associated with a specific airplane configuration, sufficient clues exist to indicate a general technique which may be applicable to similar configurations. Configurations such as externally mounted stores, pylon-mounted engines on wings, and pylon-mounted

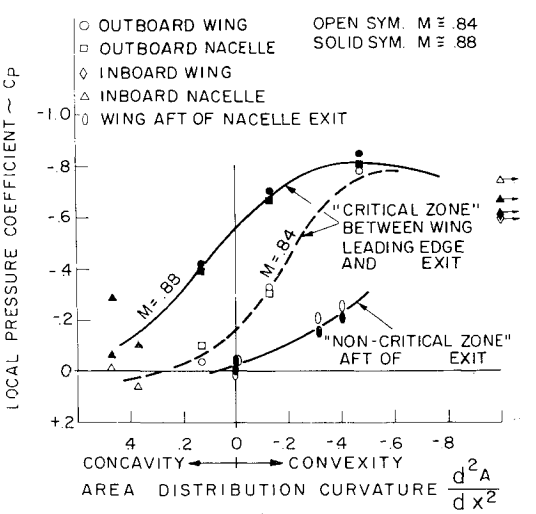

Fig. 12 Area distribution analysis correlation of local pressure level with local area distribution curvature.

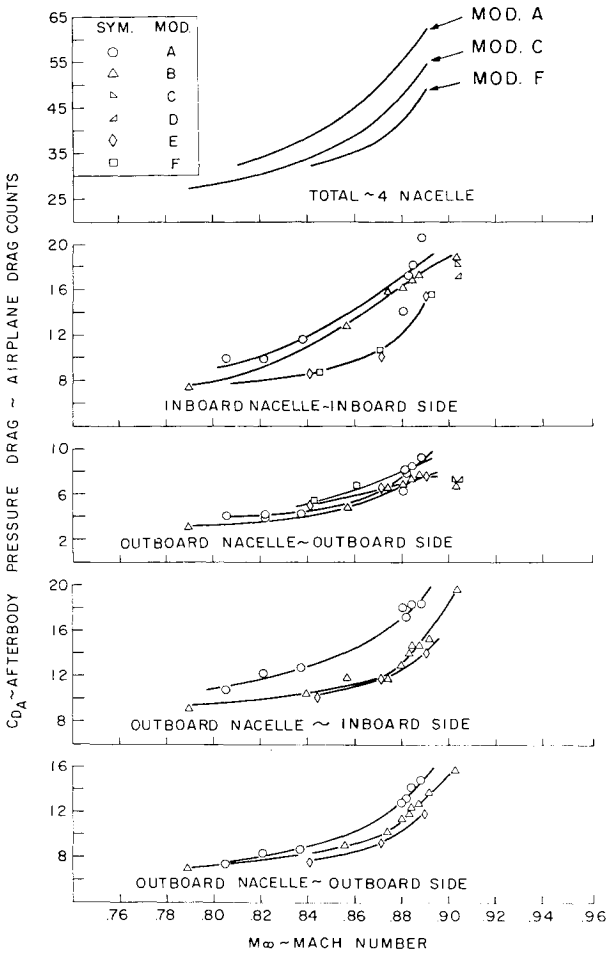

Fig. 13 Nacelle afterbody drag summary.

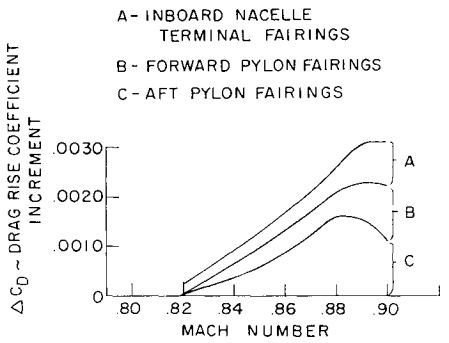

Fig. 15 Drag improvement breakdown for the best available modifications.

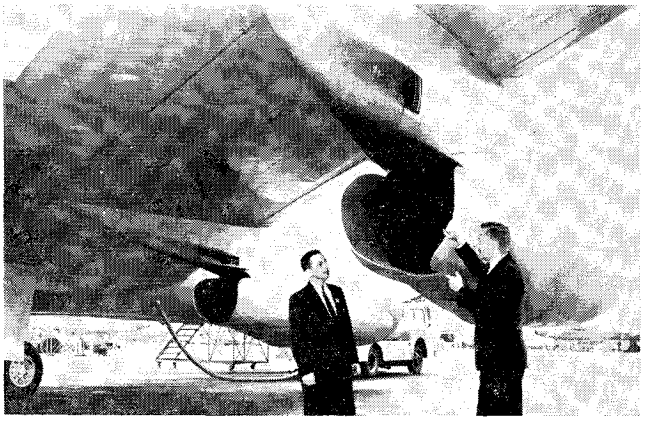

Fig. 16 Convair 990 with thickened aft pylon section and terminal fairing configuration.

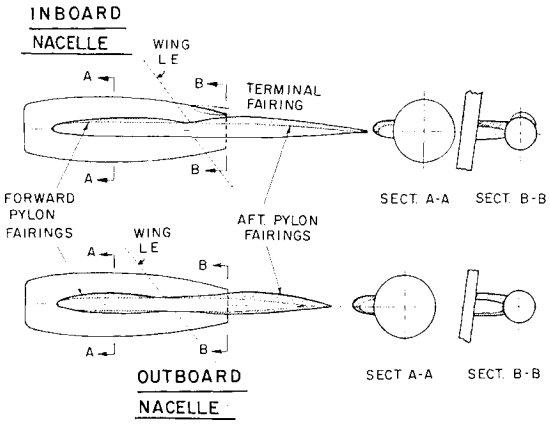

Fig. 14 Illustration of most effective configuration modification.

engines on fuselages fall into this category. The suggested methodology may be stated as follows:

1) Identification and isolation of a local transonic interference drag-rise phenomenon.

2) Evaluation of the severity of the problem and therefore the potential improvement.

3) Determination of appropriate area-distribution boundaries.

4) Definition of modifications.

Area-distribution boundaries parallel to the freestream direction (or local flow direction if the entire local system is in a wing wake for example) must be selected to include only the significant local geometry. The identification of significant and nonsignificant geometry for this purpose is admittedly a difficult task. Sound judgement based on an appreciation of the local flow phenomena must be relied upon to execute this step. Trial-and-error boundary selections which allow correlations of area distributions with either pressure distributions or drag estimates for equivalent simple bodies, such as nozzles or bodies of revolution, are suggested.

The definition of potential modifications is based upon minimizing area-distribution curvature. However, unlike the classical theory, a weighting technique must be employed. A reduction of curvature in the critical confined flow regions must be emphasized at the expense of perhaps even increased curvature in the less confined regions. No quantitative technique can be obtained with the limited data presented herein; however, the information in Fig. 12 illustrates the importance of flow confinement and may serve as a guide for similar cases.

Conclusions

1) The application of an area-rule technique to the Convair 990 nacelle, pylon-wing regions resulted in a significant drag-rise Mach number delay.

2) The method made extensive use of surface-pressure data to provide a sound basis for its application.